

# IR EMISSION FROM DUSTY WINDS — SCALING AND SELF-SIMILARITY PROPERTIES

MOSHE ELITZUR AND ŽELJKO IVEZIĆ  
*Department of Physics and Astronomy*  
*University of Kentucky*  
*Lexington, KY 40506-0055, USA*

**Abstract.** Infrared emission from radiatively heated dust possesses general scaling properties. The spectral shape is independent of overall luminosity when the inner boundary of the dusty region is controlled by dust sublimation; the only relevant property of the heating radiation is its frequency profile. For a given type of dust grains, the emission from red giants and supergiants is essentially controlled by a single parameter — the overall dust optical depth. This leads to tight correlations among different spectral properties that explain many available observations and enable systematic studies of large data bases.

## 1. Introduction

The radiation received on earth from late-type stars has undergone significant processing in the surrounding dust shell. Interpretation of the observations therefore necessitates considerable theoretical effort, involving detailed radiative transfer calculations. These calculations have traditionally required a large number of input parameters that fall into three categories:

*The Star.* Stellar input properties include the mass  $M_*$ , luminosity  $L_*$ , temperature  $T_*$  and the mass-loss rate  $\dot{M}$ .

*The Shell.* This is described by a density profile  $\rho(r)$ , defined between some inner and outer radii  $r_1$  and  $r_2$ , respectively.

*Dust Properties.* The dust abundance can be expressed via the dust-to-gas ratio  $\rho_d/\rho$ . The properties of individual grains must be specified, too, and quantities widely employed include the grain size  $a$ , the solid density  $\rho_s$ ,

sublimation temperature  $T_{sub}$  and the absorption and scattering efficiencies  $Q_{abs}$  and  $Q_{sca}$ .

Once these input properties are prescribed, they are plugged into a detailed radiative transfer calculation whose output can be compared with the observations. The most widely used output quantity is the spectral shape

$$f_\lambda = \frac{F_\lambda}{F}, \quad (1)$$

where  $F_\lambda$  and  $F$  are the observed flux density and bolometric flux, respectively. Another quantity that can be compared with observations when the angular resolution is sufficiently high is the surface brightness.

The rather large number of input parameters that had to be specified in traditional calculations creates two major practical problems. First, the volume of parameter space that must be searched to fit a given set of observations can become prohibitively large. Second, and more serious, even when a successful fit is accomplished, its uniqueness is questionable and the model parameters cannot be trusted as a reliable indication of the source actual properties.

## 2. Scaling

Much of the input required in past calculations is in fact redundant. In Ivezić & Elitzur 1995 (IE95 hereafter) we were able to show that the IR emission from late-type obeys general scaling properties that greatly reduce the number of input parameters required to fully specify the radiative transfer problem. The primary input involves only the dust, for which we must specify two types of properties: (1) Optical properties, specified through the normalized spectral shape of the extinction efficiency  $q_\lambda = Q_\lambda/Q_{\lambda_0}$ , where  $\lambda_0$  is some arbitrary fiducial wavelength; this spectral shape is controlled by the grain chemistry and size. (2) The overall optical depth  $\tau_{\lambda_0}^T$ ; this is controlled primarily by the mass-loss rate. Additional input properties have only secondary significance and involve the dust sublimation temperature,  $T_{sub}$ , the relative thickness of the dust shell  $r_2/r_1$  and the stellar temperature  $T_*$ . Note that  $T_*$  is the only stellar property that enters (and only in a secondary role). In particular, the stellar luminosity is irrelevant.

The proof of scaling is quite simple. The shell inner radius  $r_1$  is controlled by dust sublimation, namely,  $T_d(r_1) = T_{sub}$ . Introduce the dimensionless radial distance  $y = r/r_1$ . Then the radiative transfer equation becomes

$$\frac{dI_\lambda}{dy} = \tau_\lambda^T \eta(y)(S_\lambda - I_\lambda) \quad (2)$$

for  $y \geq 1$ . In this form, the equation contains no reference to either densities or dimensions. The only scale is determined by  $\tau^T$ , geometrical quantities enter only through the dimensionless radius  $y$ . The density enters only through  $\eta = n(y)/\int n(y)dy$ , its dimensionless, normalized radial profile. Because the outflows around late-type stars are controlled by radiation pressure on dust grains, the profile  $\eta$  is uniquely determined by  $\tau^T$  when the effects of gravity and dust drift are negligible (IE95). In fact, under these circumstances, the analytic expression

$$\eta \propto \frac{1}{y^2} \sqrt{\frac{y}{y-1 + (v_1/v_\infty)^2}} \quad (3)$$

provides an excellent approximation to the actual density profiles we find in our detailed numerical calculations. This function requires as additional input the ratio of initial to final velocity,  $v_1/v_\infty$ . However, this parameter has a negligible effect on the result for its typical values,  $\lesssim 0.1$ .

Additional input required is the stellar radiation. This can be specified by its flux density  $F_{*\lambda} = F_* \times f_{*\lambda}$ , where  $F_*$  is the bolometric flux. Each value of  $F_1 = F_*(y=1)$  uniquely determines a corresponding value of  $T_1$ , the dust temperature at  $y = 1$ , so the reverse is also true. And since the inner boundary is controlled by dust sublimation,  $T_{sub}$  fixes the value of  $T_1$  and through it of  $F_1$ . When the stellar luminosity varies, the shell adjusts its inner boundary so that  $F_1$  and  $T_1 (= T_{sub})$  stay the same. The radiative transfer equation is oblivious to these changes because the inner boundary always corresponds to  $y = 1$ .

These scaling properties can be generalized to arbitrary geometries and density distributions (Ivezić & Elitzur 1996). The spectral shape of dust IR emission is independent of overall luminosity when the inner boundary of the dusty region is controlled by dust sublimation; the only relevant property of the heating radiation is its spectral shape. Densities and geometrical dimensions are likewise irrelevant; they enter only through one independent parameter, the overall optical depth. The geometry enters only through angles and aspect ratios. Dust properties enter only through dimensionless, normalized distributions that describe the spatial variation of density, and the wavelength dependence of scattering and absorption efficiencies.

### 3. CONSEQUENCES

Scaling implies that for a given type of dust, the spectral energy distributions (SEDs) of late-type stars are controlled almost exclusively by overall optical depth and thus form a one-parameter family. Therefore, a single point on the normalized spectral shape  $f_\lambda$  determines the entire function and any two spectral properties should be correlated with each other. Fig-

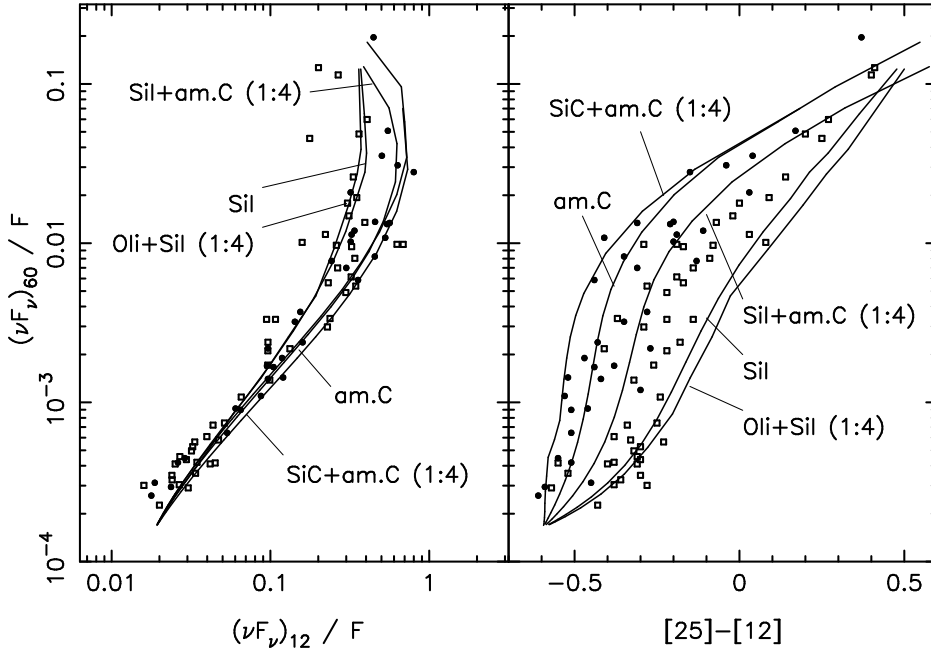
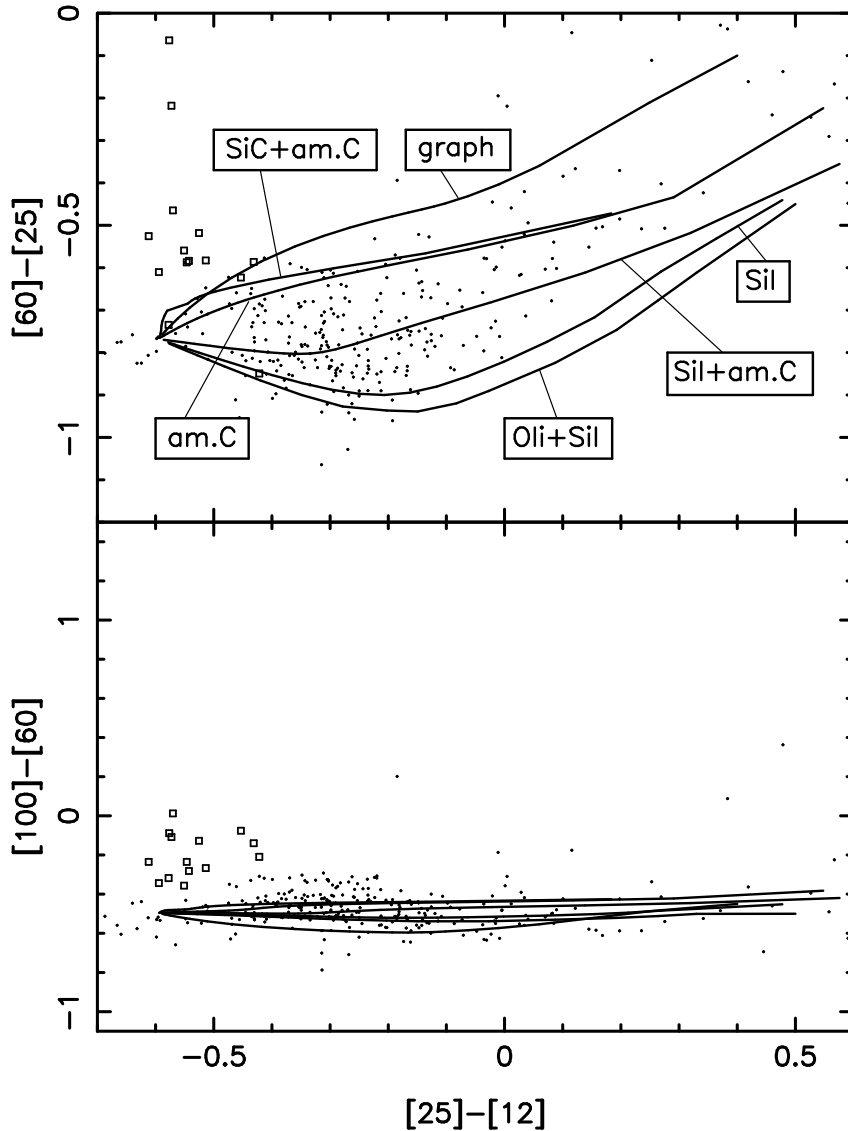


Figure 1. Test of correlations predicted by scaling. Open squares mark the data points for O-stars, solid circles C-stars. Curves describe the model predictions for various grain compositions, as marked.

Figure 1 displays in its left panel the distribution of normalized fluxes at 12 and 60  $\mu\text{m}$  for a sample of 89 stars. These are all the IRAS objects identified as late-type stars for which we were able to find listings in the literature for both total fluxes, luminosities, terminal velocities and mass-loss rates. As expected from scaling, the normalized fluxes do display a tight correlation that holds over the entire observed range, covering more than three orders of magnitude. The spread can be attributed to the differences in dust properties between carbon- and oxygen-rich stars. The right panel displays the corresponding distribution of  $(\nu F_\nu)_{60}/F$  and  $[25]-[12]$  color. The expected correlation again is evident, the separation between C and O stars is more pronounced. The lines are our computed model spectra, displaying a close agreement with the data for various relevant chemical compositions (Sil stand for astronomical silicate; am.C for amorphous carbon; Oli for olivine). The agreement between model predictions and observations is better than factor 2 in almost all cases. In addition, O-stars and C-stars clearly separate and congregate in accordance with the trend of the model curves for corresponding chemical compositions. This behavior is particularly prominent in the right panel.



*Figure 2.* IRAS color-color diagrams of all sources in the VH-window with reliable data. Solid lines represent theoretical sequences for different grain compositions, as marked. In all mixtures, the abundances ratio of the first to second component is 1:4. In the lower panel, the order of the tracks from bottom to top around  $[25]-[12] \sim 0$  is graphite, Oli + Sil, Sil, Sil + am.C, am.C and SiC + am.C.

Location in IRAS color-color diagrams has become a widely used indicator of the nature of a source. Van der Veen & Habing (1988) identified the appropriate IRAS region for late-type stars as  $[60]-[25] < 0$  and  $[25]-$

$[12] < 0.6$ , which we will refer to as the *VH-window*. Figure 2 displays the color-color diagrams for all IRAS sources with reliable data whose colors fall in this window. Our model predictions for selected grain compositions are displayed as tracks. Position along each track is determined by  $\tau^T$  and all tracks originate from the same spot,  $\tau^T = 0$ , corresponding to a black-body spectrum at 2500 K convoluted with the IRAS instrumental profiles. Distance from this common origin along each track increases with  $\tau^T$ . As  $\tau^T$  increases, the dust emission becomes more prominent and the tracks of different grains branch out. The tracks for purely Si- and C-based grains outline the distribution boundaries of most IRAS sources in the VH-window, verifying the VH conjecture that this is the color-color location of late-type stars. The data points fill the entire region between these tracks and if this spread is real, it requires a similar spread in the optical properties of the grains. This could reflect chemical mixtures, as we proposed in IE95, or perhaps grain impurities.

It is important to note that we have removed from our sample sources whose IRAS fluxes are severely contaminated by cirrus emission. This contamination is measured by the cirrus contamination index

$$CCI \equiv \frac{\text{cirr3}}{F(60)}, \quad (4)$$

where *cirr3* is the 100  $\mu\text{m}$  cirrus flux at the location of the source and  $F(60)$  is its listed 60  $\mu\text{m}$  flux. In IE95 we show that the  $[100]-[60]$  color and  $CCI$  are perfectly correlated in sources with  $CCI \gtrsim 2$ , indicating that the IRAS 60 and 100  $\mu\text{m}$  fluxes of these sources are unreliable. Sources in the upper-left corner of the color-color diagrams were thought to provide evidence for cool shells (Willems & de Jong 1986), but almost all of these sources turn out to be cirrus contaminated. Of the total 292 sources displayed in figure 2, only 11 late-type stars (4%; marked with open squares) can be identified as a group whose colors are not well explained by steady-state radiatively-driven winds. Furthermore, among these 11 sources, 10 have borderline contamination with  $1 < CCI < 2$ . Based on new simultaneous observations in a wide spectral range, Miroshnichenko et al. present in a poster paper model fits for 4 carbon stars. The results are reproduced in figure 3, showing an excellent agreement with the model for steady-state winds without any additional shells. The only parameter that varies from model to model is the visual optical depth  $\tau_v$ . Two of the displayed stars, RY Dra and VY UMa, belong to the group marked with squares in figure 2. They are borderline contaminated and show a 100  $\mu\text{m}$  excess proportional to  $CCI$ , so clearly they do not give any indication of detached shells. There is only one clearly uncontaminated C-star, U Ant, in the “cool shell” zone. Indeed, this star has a thin CO shell (Olofsson et al. 1990). We conclude

that, because of potential cirrus contamination, the SED is unfortunately not a good indicator of detached shells.

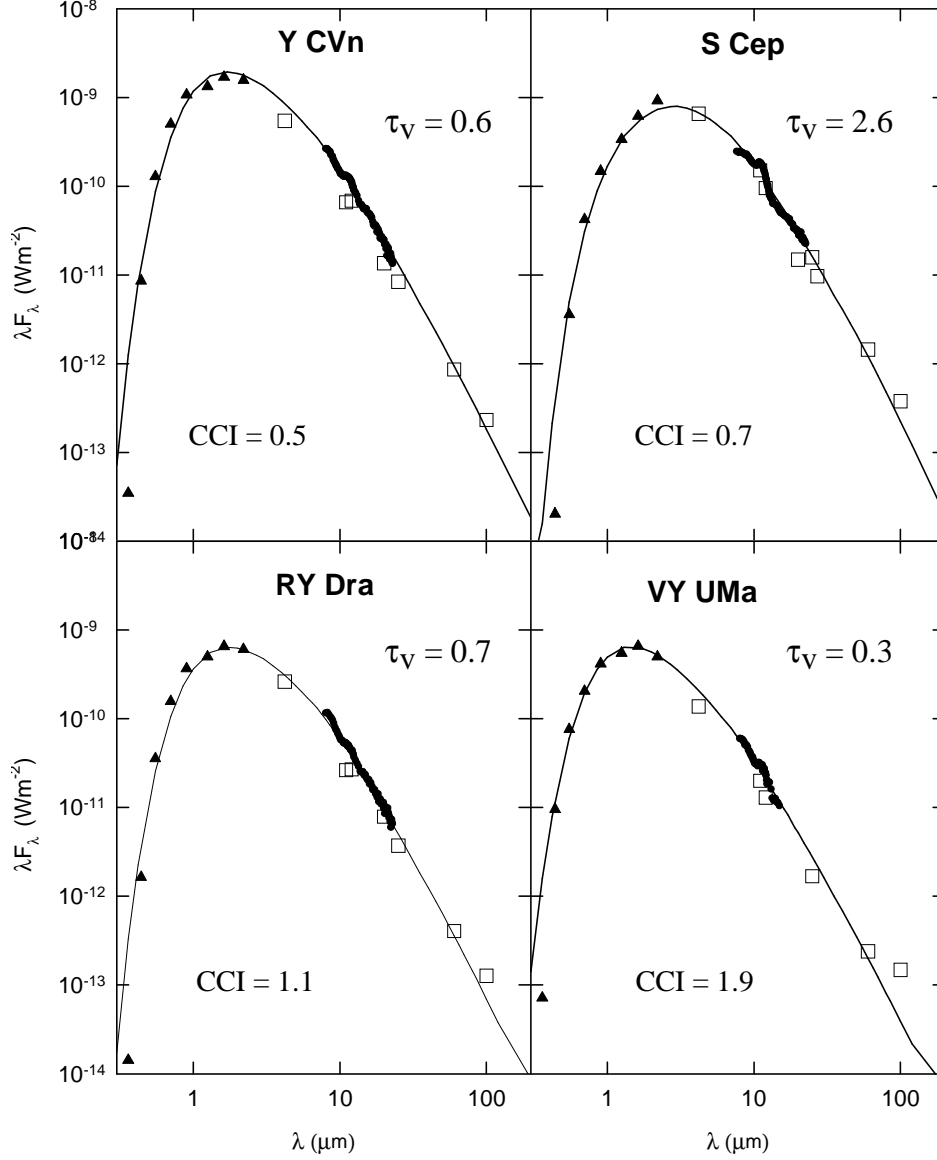


*Figure 3.* Model fits for four carbon stars with new ground based observations (triangles; Miroshnichenko & Kuratov 1996). Circles denote LRS data, squares are IRAS PSC and RAFGL data. The only adjusted model parameter is the visual optical depth  $\tau_v$ .

Thanks to scaling, the SEDs of large samples can be modeled systematically. We have embarked on a large-scale modeling project in which we

are fitting all IR data of all the late-type stars in the IRAS catalogue ( $\sim 5,000$  sources). The outcome of this project will be a supplemental catalogue, listing the optical depths and dust properties of the largest sample yet modeled with a single, consistent approach.

#### 4. CONCLUSIONS

The structure displayed in infrared color-color diagrams is a result of general scaling properties of radiatively heated dust. Sources segregate into families that differ from each other because of dust properties, not because of the central source. Within family, location of each source is controlled by its optical depth. Concerning late-type stars — properly selected IRAS data is almost fully explained by steady-state winds. The spectral shapes of sources free of cirrus contamination do not give evidence for detached shells in more than a handful of sources.

Support by NASA grant NAG 5-3010, NSF grant AST-9321847 and the Center for Computational Sciences at the University of Kentucky is gratefully acknowledged.

#### References

- Ivezić, Ž., Elitzur, M., 1995, ApJ, 445, 415 (IE95)
- Ivezić, Ž., Elitzur, M., 1996, MNRAS (submitted)
- Miroshnichenko, A. & Kuratov, K., 1996, unpublished
- Olofsson, H. et al., 1990, A&A, 230, L13.
- van der Veen, W.E.C.J., & Habing, H.J. 1988, A&A, 194, 125.
- Willems, F.J., & de Jong, T. 1986, ApJ, 309, L39.